Check for updates

Pressure-induced phase transition of 1,5-diamino-1H-tetrazole (DAT) under high pressure†

Cheng Jin, [ID] ‡[a] Ying Liu,‡[b] Lijuan Wang,[a] Weijing Zhang,[c] Tonglai Zhang [ID] *[c] and Jinlong Zhu *[ad]

Nitrogen-rich energetic materials have attracted certain interest as promising high energy density materials (HEDMs) in recent years. Pure N_2 and nitrogen-based molecular crystals are ideal HEDMs that would polymerize under high pressure, as reported in previous literature. We selected a 1,5-diamino-1H-tetrazole (DAT) crystal, which has two kinds of molecular structures and hydrogen bonds, to study under high pressure by spectroscopy and diffraction due to its high nitrogen percentage and low sensitivities. Pressure-induced structure transitions occur at pressures of 2.3–6.6 GPa, ~8.5 GPa, and ~17.7 GPa. The phase transition at 2.3–6.6 GPa is related to the rotation of NH_2, and the latter two transitions are caused by both the rotation of NH_2 and the distortion of the heterocycle. Significantly, the reconstitution of the hydrogen bond may induce the rotation/distortion of the NH_2/heterocycle in the second phase transition. There is no evidence showing a transformation between the two molecular structures in the whole pressure range studied. Our investigation uncovers the phase transition mechanism of DAT under pressure, which will help to find targeted HEDMs.

Introduction

High energy density materials (HEDMs) are defined as those that release tremendous heat and/or vast amounts of gas in a very short time by heat, impact, shock, spark, *etc.* stimulation. They can broadly be classified as pyrotechnics, propellants (including gas generators) and explosives, which are widely used in daily life, aerospace and the military.[1-6] In general, HEDMs are expected to have high energetic density, low sensitivity and release less greenhouse gas than conventional energy materials.[1,2,4,5] Typical HEDM representatives are trinitrotoluene (TNT), 1,3,5,7-tetranitro-1,3,5,7-tetrazacyclooctane (HMX), 1,3,5-trinitrohexahydro-s-1,3,5-triazine (RDX) and nitrogen-rich energetic materials chronologically. The instant pressure can go up to 50 GPa and temperature can go up to 5500 K during the explosion and combustion of HEDMs, resulting in molecular polymorphs and/or crystal phase transitions.[1,7,8] As an effective tool, high-pressure technology can simulate a certain degree of explosion and combustion, such as the possible formation of

dimers, trimers, or new polymer polymorphs. Furthermore, high-pressure may lead to the formation of hydrogen bonds,[9] which will significantly change the sensitivity of HEDMs. Therefore, investigating the phase evolution and the decomposition of HEDMs under high pressure is critical to fundamentally understand explosion and combustion processes, and it will be helpful to find a potential pathway for designing new energetic materials.[4,7] Recent experimental and theoretical efforts to find a more stable crystal structure hosting higher energetic density and lower sensitivity have focused on aspects of chemical composition, molecular structure and intermolecular interactions.[2,4-6] Remarkably, nitrogen-rich energetic materials have attracted considerable interest due to their high nitrogen content, low carbon content, heterocyclic structure and hydrogen bond that exists among molecules.[2,4-6,9,10] Among the nitrogen-rich energetic materials, polymeric nitrogen characterized by pure single nitrogen bonding has attracted lots of attention because of the expected large energy release during the process of single-bond (~160 kJ mol^{-1}) rupture and triple-bond (~946 kJ mol^{-1}) formation.[11,12] Moreover, the gaseous product is pure N_2, an environmentally friendly counterpart. Eremets *et al.* reported that polymeric cubic *gauche* nitrogen (cg-N) was obtained using pure N_2 as a precursor in a laser-heated diamond anvil cell (DAC) under the pressure 110 GPa and temperature higher than 2000 K at 2004.[11] More recently, black-phosphorus-structured nitrogen (BP-N) was synthesised by Laniel *et al.*[13] and Cheng Ji *et al.*[14] under 140 GPa, ~4000 K and 146 GPa, >2200 K in DACs. However, the phase transitions from N_2 to cg-N or BP-N require a pressure higher than 110 GPa and

^{a}*Center for High Pressure Science and Technology Advanced Research (HPSTAR), Beijing, 100094, China. E-mail: zhujl@sustech.edu.cn*

^{b}*Xi'an Modern Chemistry Research Institute, Xi'an, 710065, China*

^{c}*State Key Laboratory of Explosion Science and Technology, Beijing Institute of Technology, Beijing, 100081, China. E-mail: ztlbit@bit.edu.cn*

^{d}*Department of Physics, Southern University of Science and Technology, Shenzhen, 518055, China*

† Electronic supplementary information (ESI) available. See DOI: 10.1039/d0ra06328b

‡ Contributed equally to this work.

temperature higher than 2000 K, while both of them transfer back to N_2 once they are released to ambient pressure. For practical application, the primary task is to achieve the phase transition at ambient pressure or at least pressure below 30 GPa, which could be realized in a large volume press. One of the possible solutions could be hydrogen bonds formation among molecules, as they play a key role of maintaining the stability of the crystallographic structure and leading to a higher density phase with insensitivity.[15–20] More importantly, pressure can easily tune the hydrogen bond by means of rearrangement,[21] reconstruction[22] and symmetrization.[23] In this work, 1,5-diamino-1*H*-tetrazole (DAT), a member of heterocyclic nitrogen, was selected for the highest nitrogen content (84%) by weight compared with tetrazole and 5-amino-tetrazole (5-AT). It is abundant of nitric single-bonds ($\sim$160 kJ mol^{-1}) and double-bonds ($\sim$419 kJ mol^{-1}), which is easier to polymerize compared to a triple-bond ($\sim$946 kJ mol^{-1}) under pressure. Generally, theoretical[26] and experimental[27] researches reported two kinds of DAT molecule polymorphs at ambient conditions, which are denoted as molecular structure I and structure II in Fig. 1(a), respectively. The tetrazole ring is planar within 0.001 (1) Å and a π-system exists on the tetrazole ring. The N5–H or N5H_2 group is lying in the tetrazole ring plane and conjugated with the π-system of the tetrazole ring, while N6H_2 is not the case.[24] At ambient conditions, with hydrogen bonds of N–H···N in the framework, DAT crystallized in a high-density structure with a space group $P2_1/c$ and lattice parameters of $a = 6.780(1)$ Å, $b = 6.112(1)$ Å, $c = 10.694(1)$ Å, and $\beta = 107.25(1)°$.[24] The schematic crystal structure is plotted in Fig. 1(b). The unique three-dimensional network has hydrogen bonds between layers, resulting in a slight rotation of the molecule. This makes the structure more stable and insensitive. Lesnikovich *et al.* reported the melt temperature and decomposition temperature of DAT are 460 K and in the range of 470 K to 540 K, respectively. The enthalpy change of the decomposition of DAT is 850 kJ mol^{-1} compared to 220 kJ mol^{-1} of 1-methyl-5-aminotetrazole (MAT), indicating that DAT has a better thermal stability and is more energetic releasing. Besides, DAT releases gas up to 550 cm^3 g^{-1} during the decomposition, while it is just 240 cm^3 g^{-1} for MAT.[25]

In Lesnikovich's another work under high temperature,[26] molecular DAT will partially transform from structure II to structure I when heated under 500 K by transferring the hydrogen on the N4 atom to the –N5H bonded to the C atom. In the progress of heating to 900 K, molecule in structure I would firstly break the N1–N2 and N3–N4 bonds to produce an intermediate product CN$_4$H$_4$, releasing N_2 gas. Then, CN$_4$H$_4$ decomposes to HCN, NH_3, and N_2 through hydrogen transferring between amino, C–N&N–N bond rupture and C–H bond formation.[26] The remaining molecule in structure II will first break the C–N4 and N1–N2 bonds and produce CN$_3$H$_3$ and HN$_3$ when heated to 900 K. CN$_3$H$_3$ subsequently decomposes to 1,2,4-triazole (C$_2$N$_3$H$_3$) with releasing N_2 and NH_3. Lesnikovich reported the possible DAT decomposition routes under high temperature, but the crystal structure transition of DAT under high pressure still needs to be explored further.

In this work, the possible structural phase transition of DAT polymorphs under pressure is investigated by *in situ* Raman, Infrared-Ray (IR) spectra and X-ray diffraction (XRD) experiments up to 40 GPa. The results indicate that three crystal structure phase transitions occurred at the pressure of 2.3–6.6 GPa, $\sim$8.5 GPa and $\sim$17.7 GPa, respectively. The rotation of NH_2 induces the first phase transition. Both rotation of NH_2 and distortion of heterocycle are involved in the second and third transitions. The transition at $\sim$8.5 GPa is closely related to the reconstitution of the hydrogen bonds. No obvious evidence shows the molecular transformation between the two molecular structures.

Experimental methods

DAT samples were synthesized by reacting thiosemicarbazide, sodium azide, and ammonium chloride in dimethylformamide in the presence of PbO. The detailed information can be found in ref. 28. Elemental analyses (C, H and N) were performed on a Flash EA 1112 fully automatic trace element analyzer. The samples of DAT were dried in the water bath drying oven at 60 °C for 24 h and cooled to room temperature in dryer before the test. Through elemental analyses, we got the percent of C and N as 12.56% and 83.76%, respectively. X-ray powder diffraction (XRPD) measurements at ambient pressure were performed on a Bruker D8 advance diffractometer at 60 kV, 300
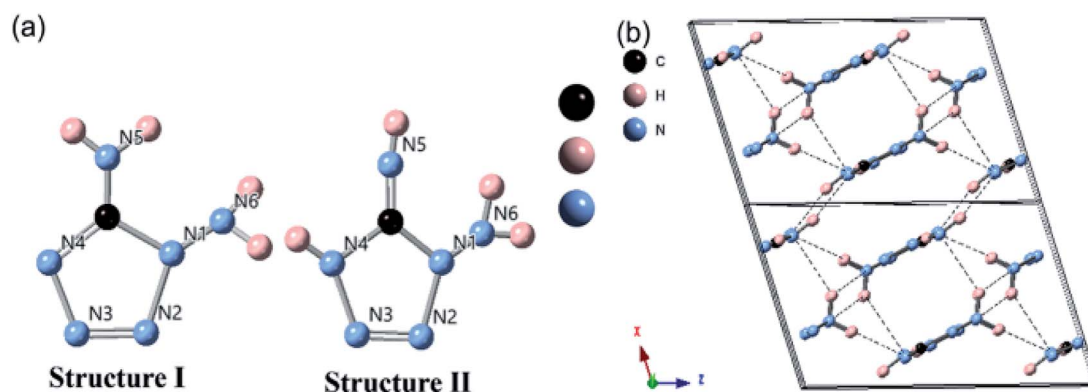

Fig. 1 (a) Polymorphs of 1,5-diamino-1*H*-tetrazole are denoted as structure I and structure II, (b) crystal structure of 1,5-diamino-1*H*-tetrazole at ambient conditions. The dashed blue lines represent the hydrogen bonds.

mA and Cu Kα radiation ($\lambda = 1.5406$ Å), with a scan speed of 5 °C min^{-1} and a step size of 0.02° in 2θ. The XRPD result and the simulated XRD peaks from cif file of ref. 24 are plotted in Fig. S1.† Therefore, we propose that the purity was higher than 95%. High-pressure experiments were carried out in a DAC with diamond culets of 300 μm in diameter. A T301 stainless steel gasket was used and pre-indented to 26 μm in thickness, and then a hole of 100 μm in diameter was drilled into the centre as the sample chamber. Ruby balls with a size of 10 μm in diameter were used to monitor the pressure during the experiments.[29–31] The measurement point is about 3 μm from the ruby ball. No pressure transmission medium was used because DAT is a soft crystal with a bulk modulus of 23(3) GPa fitted as below, which can keep the sample chamber in a quasi-hydrostatic condition.

The *in situ* Raman experiments were performed using a Renishaw Invia. The excitation wavelength of the laser was 532 nm. Raman spectra were collected through a holographic grating of 2400 g per mm. The laser power range was from 0 to 20 mW (100%) to avoid damaging the DAT sample. The strong peak of diamond was located at 1300–1400 cm^{-1} and 2300–2700 cm^{-1}, which was cut off for all the data in Raman.

The IR spectra were collected on a Bruker VERTEX 80v FTIR spectrometer with a HYPERION 2000 IR microscope. The IR beam was set to the size of 20 × 20 μm by a pair of knife-edge diaphragms. KBr pellet was used to optimize the thickness of the sample. The IR spectra were collected in transmission mode with a resolution of 4 cm^{-1} and recorded with a nitrogen-cooled broadband mercury cadmium telluride detector.

The high-pressure XRD experiments were conducted with a symmetric DAC with same geometry and same culet of 300 μm comparing to the DAC in Raman experiment, and similar procedures to the Raman measurements were adopted. The high-pressure XRD experiments were performed at the 4W2 High Pressure Station of Beijing Synchrotron Radiation Facility (BSRF) where the X-ray wavelength was $\lambda = 0.6199$ Å. The XRD patterns were collected with a MAR 3450 image plate detector and integrated from the images using the FIT2d software.

Results and discussion

X-ray diffraction of DAT under pressure

To investigate the phase transitions of DAT under pressure, synchrotron XRD pattern was collected up to 40 GPa, as plotted in Fig. 2. Through checking the full width at half maxima (FWHM) of peak at 002, a new peak near 002 is found at 2.3 GPa. At 6.2 GPa, there is a peak near 013 emerging. At 9.6 GPa, a new peak at 2 theta of 7.7° is observed. At 17.1 GPa and 19.7 GPa, a new peak at 2 theta of 7.2° and a shoulder at 2 theta of 7.5° appear. The vanishings of peaks are also marked by black arrows. From the above observation, there may exist three phase transitions roughly at 2.3–6.2 GPa, 9.6 GPa and 17.1–19.7 GPa. Under further compression, amorphization occurs when pressure is higher than 27.3 GPa. By adopting the ambient pressure phase,[24] we refined the XRD data by Le Bail method and fitted the bulk modulus using 2nd-order Birch–Murnaghan (BM) equation of state (EOS) in low pressure phase, which got the
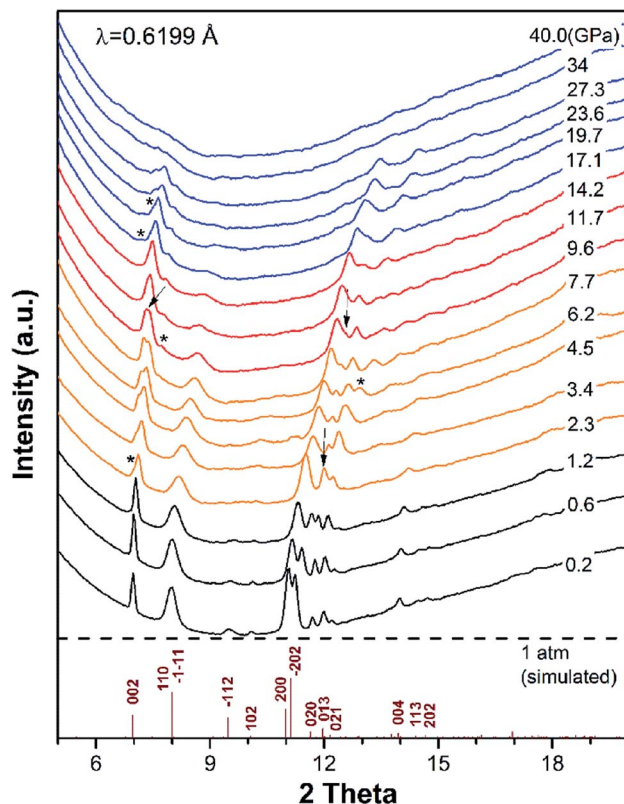

Fig. 2 XRD of DAT under pressure. The asterisks mark the new peaks. The arrows highlight the peak vanishings. The black, orange, red and blue lines stand for the phase I to phase IV.

bulk modulus $B_0 = 23$ (3), as shown in Fig. S2 and S3.† The derivative of bulk modulus is set as $B'_0 = 4$ and the original volume of crystal is 423.2 Å^3 in ref. 24. The detailed information about refinement of XRD data and fitting of B_0 for ambient pressure phase is shown in the ESI.† The fitting result shows that DAT is a soft crystal under low pressure, which can keep the sample chamber in a quasi-hydrostatic condition.

Raman and IR spectroscopy under pressure

To investigate the source of possible phase transitions, *in situ* Raman and IR experiments under pressure were carried out. They can provide the information of local vibration and bonding under pressure. Raman/IR spectra of DAT at near ambient pressure (0.03 GPa) and decompression to near ambient pressure are displayed in Fig. S4 and S5.† The details of vibration modes at ambient conditions are listed in Table S1† and are compared with the IR spectra modes in ref. 26 and 32. Some modes are recognized according to ref. 33 and 34. Totally, the new found peaks at 50–200 cm^{-1} are recognized as lattice modes. The modes located in 200–1000 cm^{-1} and 3000–3500 cm^{-1} are related to NH$_2$ stretching (ν(NH$_2$)) or N–H wagging (γ(N–H)). The modes in 1000–1800 cm^{-1} are mostly connected with heterocycle vibration, plus the N–H bending modes (β(N–H)) at 1545 cm^{-1} in Raman and at 1636 cm^{-1}, 1659 cm^{-1} in IR.[34,35] In Fig. S4 and S5,† the unique vibrational modes of structure I and structure II can both be found, indicating the two typed of DAT polymorphs coexist in

the sample. It should be noticed that XRD pattern shows a pure phase at ambient phase because both of the DAT polymorphs can exist in the same crystal.[26,27] There are no direct connection between crystal structure and molecular structure. The detailed identification is shown in the supplemental materials. Certain unique vibrational modes of two molecule structures can be observed with pressure up to 40 GPa, such as $\nu_{endo}(C{=}N)$ (in-phase) at 1473 cm^{-1} in molecular structure I and $\nu_{exo}(C{=}N)$ at 1669 cm^{-1} in molecular structure II. No obvious evidence shows molecular structure transformation occurs accompanying the crystal structure phase transitions. Finally, almost all the modes recover when decompressing to ambient pressure in Fig. S4 and S5,† indicating the local chemical environment is preserved.

Fig. 3 and 4 plot the representative Raman/IR spectra of DAT under pressure up to 40 GPa, and the relative peak shifts of the Raman and IR modes as a function of the pressure are plotted in Fig. 5 and 6, respectively. It has to be noticed that the Raman peak at 791 cm^{-1} is too strong to be plotted in Fig. 3, we only plotted its pressure evolution in Fig. 5. Furthermore, the Raman modes at 90 cm^{-1}, 147 cm^{-1}, 328 cm^{-1}, 687 cm^{-1}, 1134 cm^{-1} and IR mode at 1730 cm^{-1} vanish once increasing pressure, so they are not plotted in Fig. 5 and 6. Under pressure, the lattice modes in 50–200 cm^{-1} have significant anomalies at 2.3–6.6 GPa. In Fig. 3(a), at 2.3 GPa two new modes located at 75 cm^{-1} and 105 cm^{-1} emerge. When compressing to 3.5 GPa, two shoulders at 84 cm^{-1}, 104 cm^{-1} and a peak at 178 cm^{-1} appear. At 4.8 GPa, a shoulder is observed at 96 cm^{-1}. These indicate the first phase transition from phase I to phase II in the pressure range between 2.3 GPa and 6.6 GPa, which is consistent with the XRD results. Meanwhile, molecular vibrations also show complex changes. In Fig. 3, at 2.3 GPa a new mode emerges at 689 cm^{-1}. The $\nu(C{-}NH_2)$ mode at 495 cm^{-1} broadens and splits into two peaks at 490 cm^{-1}, 498 cm^{-1} under pressure of 3.5 GPa. At 6.6 GPa, $\nu(NH_2)$ mode at 697 cm^{-1} splits into two modes at 719 cm^{-1}, 729 cm^{-1} and a new peak near the $\beta(N{-}H)$ is observed at 1556 cm^{-1}. In Fig. 4, when compressed to 2.7 GPa, a new mode at 662 cm^{-1} appears and a new peak at 1608 cm^{-1}
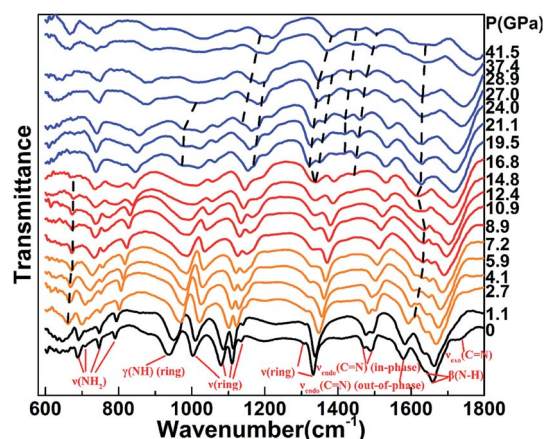

Fig. 4 IR spectroscopy of DAT as a function of pressure up to ∼40 GPa. The black, orange, red and blue lines stand for the phase I to phase IV. The dash lines mark the new modes and their evolution. And other marks of the vibrational modes are same to the Raman spectra in Fig. 3.

between the $\nu_{endo}(C{=}N)$(out-of-phase) and $\beta(N{-}H)$ mode can be found. Summarly, all the above anomalies occur in the vibrational range of NH$_2$ stretching or just near the bending mode of N–H. The interaction between molecules becomes stronger with compression, as expected, the amino attached to the hetero-cycle is easily to be tuned and rotate under pressure. This is because the amino group attached on the N1 in DAT is not conjugated with the π-system, as that in a tetrazole ring.[24] Therefore, at 2.3–6.6 GPa the phase transition is related to the rotation of NH$_2$, much like the reported rotation of NO$_2$ of in HMX that induced the phase transition at ∼5.0 GPa in ref. 7. This phase transition is sluggish over a broad pressure range. It may be caused by their Gibbs free energy difference or the slow transition kinetics.[7,9]

With the pressure increasing, obvious changes of vibration modes are observed at ∼8.5 GPa. In the lattice modes, the peak at 104 cm^{-1} gets broadening with an obvious red shift and splits
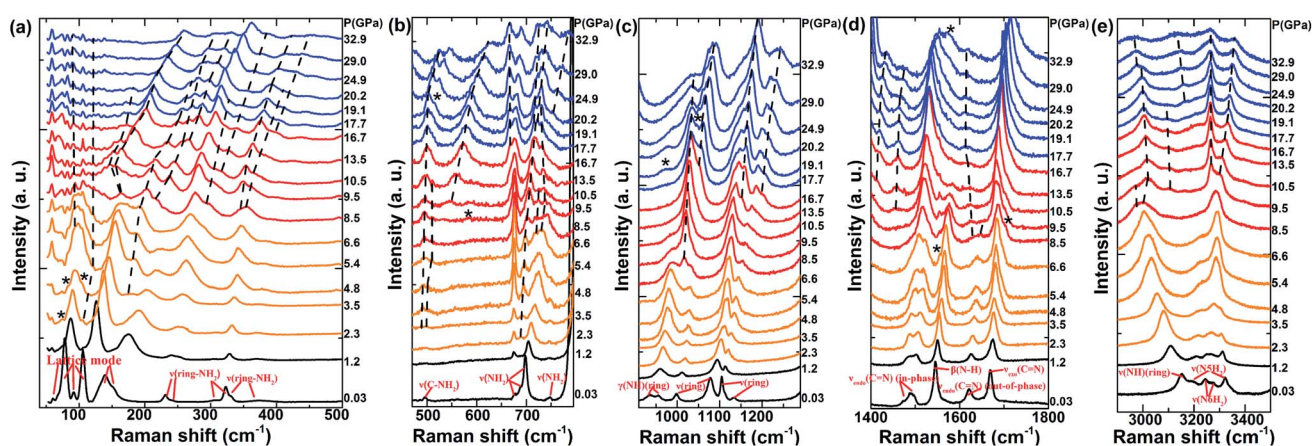

Fig. 3 Raman spectroscopy of DAT as a function of pressure up to ∼40 GPa. (a) 50–500 cm^{-1}, (b) 500–800 cm^{-1}, (c) 800–1300 cm^{-1}, (d) 1400–1800 cm^{-1}, (e) 2950–3450 cm^{-1}. The black, orange, red and blue lines stand for the phase I to phase IV. The asterisks and dash lines mark the new modes and their evolution. The subscript "exo" refers to the mode attached to the five-membered nitrogen heterocycle. The subscript "endo" refers to the modes inside the five-membered nitrogen heterocycle. ν refers to stretching of bond. β refers to bending of bond. γ refers to wagging of bond. The ring with bracket behind modes, such as $\gamma(N{-}H)$(ring), means that H is attached to the heterocycle directly.
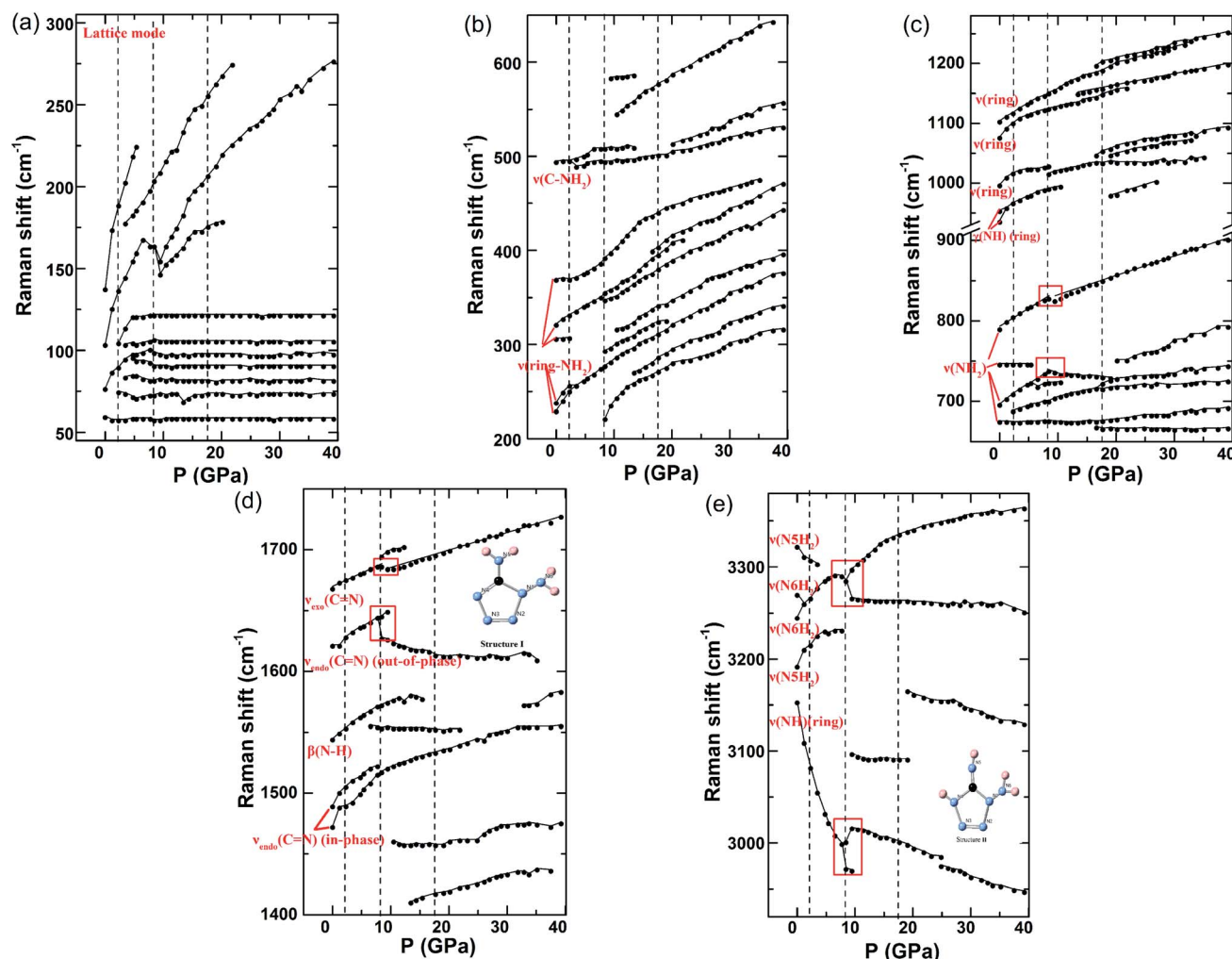
Fig. 5 Evolution of Raman vibration modes upon increasing pressure. (a) The lattice mode in 50–300 cm^{-1}, (b)–(e) contain the evolution of molecular modes, (b) 200–6500 cm^{-1}, (c) 650–1250 cm^{-1}, (d) 1400–1750 cm^{-1}, (e) 2950–3350 cm^{-1}. The dash lines mark the phase transition pressure points. The red squares mark significant discontinuities at ∼8.5 GPa, which can be the evidence of the reconstitution of hydrogen bonds.

into two peaks at 147 cm^{-1}, 155 cm^{-1} under the pressure of 9.5 GPa, corresponding to the changes in XRD pattern near 9.5 GPa. This indicates the second phase transition from phase II to phase III. Meanwhile, anomalies of molecular vibrational modes can also be found. In Fig. 3, under pressure of 8.5 GPa two new modes at 222 cm^{-1} and 294 cm^{-1} emerge, and the ν(ring-NH$_2$) at 322 cm^{-1} and ν(N–H)(ring) at 3154 cm^{-1} broaden and split. At 9.5 GPa, a new peak is observed at 3098 cm^{-1} and ν(N6H$_2$) mode at 3246 cm^{-1} splits into two peaks at 3267 cm^{-1} and 3298 cm^{-1}. Under pressure up to 10.5 GPa, a shoulder and a new peak emerge at 317 cm^{-1}, 546 cm^{-1}, respectively. Overall, the emergence and splitting of modes stated above are in the region of NH$_2$ stretching or N–H wagging, indicating NH$_2$ rotation involves in the second phase transition.[7] However, different from changes at 2.3–6.6 GPa, the anomalies at ∼8.5 GPa are not only related to the NH$_2$ vibrations but also located in the range of heterocycle vibrations. Several modes related to heterocycle disappear. For instance, in Fig. 3(c), ν(ring) mode at 998 cm^{-1} disappears above 8.5 GPa. In Fig. 4,

ν_{endo}(C=N)(out-of-phase) at 1578 cm^{-1} vanishes when pressure is higher than 8.9 GPa. There are also new modes emerging in the range of heterocycle vibrations. In Fig. 3, under the pressure of 8.5 GPa two new modes emerge at 1017 cm^{-1} and 1695 cm^{-1}. At the same pressure, the ν_{endo}(C=N)(out-of-phase) mode at 1622 cm^{-1} splits into 1628 cm^{-1} mode and 1646 cm^{-1} mode. A new peak at 1461 cm^{-1} is observed at 10.5 GPa. These anomalies lying in the range of heterocycle vibrations indicate that the second phase transition is also accompanied by the heterocycle distortion. As further increasing pressure, the repulsive force occurring between π-system of tetrazole rings may make the heterocycle distortion.[9] A similar phenomenon is also reported in ref. 7 where the distortion of the C$_4$N$_4$ ring in HMX induces phase transitions under pressure up to 40 GPa. Another example is that the distortion of heterocycle in tetrazole also occurs in the phase transition under pressure of 3.1–7.8 GPa, which is induced by the formation of hydrogen bonds.[9] The influence of hydrogen bonds on this transition will be discussed
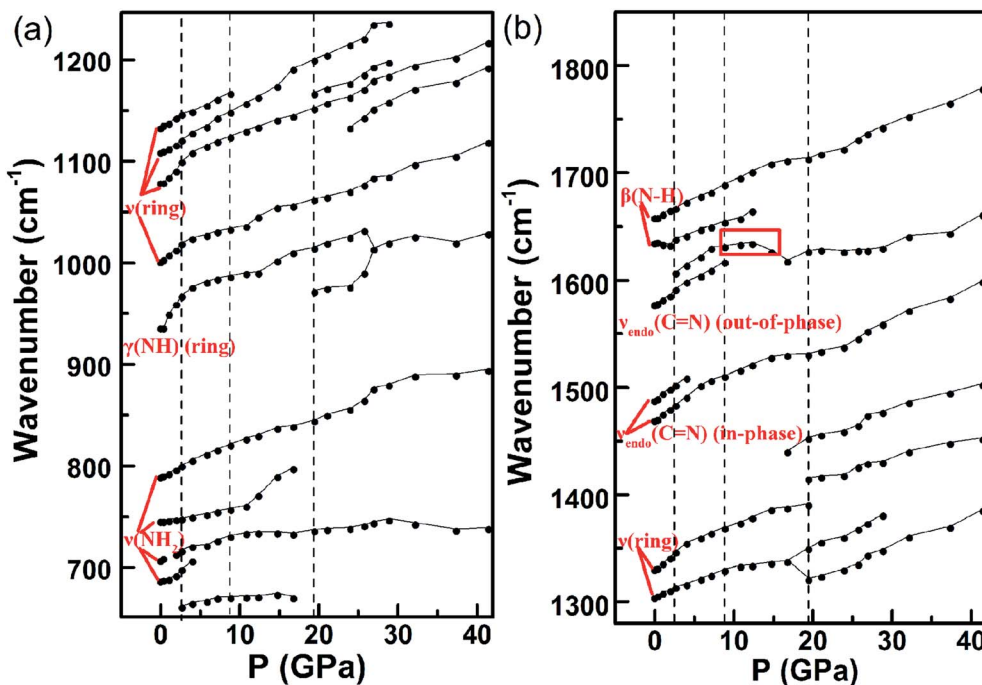
Fig. 6 Evolution of IR vibration modes upon increasing pressure. (a) 650–1250 cm^{-1}, (b) 1300–1850 cm^{-1}. The dash lines mark the phase transition pressure points. The red squares mark the significant discontinuities at ~8.5 GPa.

in the following section. In a word, the phase II to phase III transition is from both NH$_2$ rotation and heterocycle distortion.

Further compression to 13.5 GPa, some changes occur in molecular vibrations. For example, new peaks at 271 cm^{-1}, 1151 cm^{-1}, 1411 cm^{-1} appear in Fig. 3. On the contrary, XRD peaks in Fig. 2 and lattice modes in Fig. 3 have no obvious changes at this pressure point. Therefore, these anomalies can only be recognized as local vibration changes without phase transition. By further compression, significant anomalies of molecular vibrational modes are observed at ~17.7 GPa. Although no obvious changes are observed in lattice modes, the anomalies in XRD peaks and molecular vibrations confirm the phase transition from phase III to phase IV. Firstly, several NH$_2$ vibration modes disappear. In Fig. 3, the peak at 3098 cm^{-1} emerging at 9.5 GPa disappears above 19.1 GPa. The shoulder at 294 cm^{-1} which is observed at 8.5 GPa vanishes when pressure is higher than 19.1 GPa. In Fig. 4, the peak at 662 cm^{-1} which appears at 2.7 GPa and the ν(NH$_2$) mode at 747 cm^{-1} both vanish when pressure is higher than 16.8 GPa. Meanwhile, new modes of NH$_2$ vibrations are observed. In Fig. 3, two shoulders emerge at 400 cm^{-1} and 669 cm^{-1} around 16.7 GPa. When compressed to 17.7 GPa, the mode at 689 cm^{-1} which appears under the pressure of 2.3 GPa splits into two peaks. At 19.1 GPa, a new peak can be found at 3166 cm^{-1}. A shoulder at 514 cm^{-1} and a peak at 752 cm^{-1} appear at 20.2 GPa. In Fig. 4, a new mode at 973 cm^{-1} appears near the γ(N–H)(ring) mode at 19.5 GPa. Similar to the phase transition at ~8.5 GPa, the changes above show that NH$_2$ rotation is mainly responsible for the phase transition at ~17.7 GPa.[7] Also, heterocycle vibration vanishings are observed in this transition, such as the ν(ring) at 1332 cm^{-1} disappearing near 19.5 GPa in Fig. 4. At the same

time, a number of new peaks related to heterocycle vibration can be found: in Fig. 3, two shoulders at 1048 cm^{-1} and 1198 cm^{-1} emerge at 16.7 GPa; near 19.1 GPa, a peak appears at 1048 cm^{-1} marked by an asterisk. In Fig. 4, a new peak is observed at 1441 cm^{-1} around 16.8 GPa; two modes emerge at 1168 cm^{-1}, 1416 cm^{-1} and the ν(ring) mode at 1305 cm^{-1} splits near 19.5 GPa. These changes about heterocycle vibrations indicate that distortion of heterocycle also involves in this phase transition.[7,9] We conclude that the third phase transition is induced by both rotation of NH$_2$ and distortion of heterocycle.[7,9]

Further increasing the pressure, some more anomalies in molecular modes occur at ~24.9 GPa, including a new peak at 2976 cm^{-1} near 24.9 GPa in Fig. 3 and another new peak at 1134 cm^{-1} under 24.0 GPa in Fig. 4. These may be from the disordering entangled amorphization or local molecular vibration changes.

The influence of hydrogen bonds

Just as stated above, hydrogen bond has a significant impact on the structure and phase transition of HEDMs under pressure.[15–23] Coincidentally, large amount of hydrogen bonds exist in the crystal of DAT as shown in Fig. 1(b). Under compression, most modes in both vibrational spectra exhibit blue shifts with the increasing of pressure before phase transitions, as the intra- and inter-atomic distances shrink under compression.[9] However, in Fig. 5(e) ν(N–H)(ring) at 3154 cm^{-1}, ν(N6H$_2$) at 3271 cm^{-1} and ν(N5H$_2$) at 3323 cm^{-1} exhibit red shifts as the result of the hydrogen bond interaction.[26] Pressure shortens the distance of H⋯N in the hydrogen bonds and strengthens electrostatic attraction, therefore extending the N–H bond length and resulting in the red shifts.[37] On the contrary, ν(N6H$_2$)

at 3246 cm^{-1} and ν(N5H$_2$) at 3193 cm^{-1} exhibit blue shifts. The same phenomena occur in the Cui's work[9] on tetrazole and Zou's work[36] on urea nitrate under pressure. This is because the attractive and repulsive interactions coexist in the proton donor and acceptor of hydrogen system.[9,36] So the blue and red shifts are determined by the percentage of attractive and repulsive interaction.

During compression, significant discontinuities occur in the second phase transition at ∼8.5 GPa. Several sudden droppings of frequency and red shifts are observed in Fig. 5 and 6, which are marked by red squares. More specifically, in Fig. 5, the ν(NH$_2$) mode at 729 cm^{-1}, which is split from the ν(NH$_2$) mode at 697 cm^{-1} under 6.6 GPa, transforms from blue shift to red shift near 8.5 GPa. At the same pressure, the new peak at 1628 cm^{-1} which is split from ν_{endo}(C=N)(out-of-phase) mode at 1622 cm^{-1} shows a huge reduction of frequency comparing to the original mode and exhibits a red shift. When compressed to 9.5 GPa, the ν(NH$_2$) mode at 791 cm^{-1}, the ν_{exo}(C=N) mode at 1669 cm^{-1} show a sudden frequency dropping, and the peak at 3267 cm^{-1} splitting from ν(N6H$_2$) mode at 3246 cm^{-1} not only has a large frequency dropping comparing to the original mode but also shows a red shift. In Fig. 6(b), the mode at 1608 cm^{-1} emerging at 2.7 GPa gradually transforms from blue shift to red shift near 8.9 GPa.

Generally speaking, sudden drops of frequency in the vibration modes indicate the releasing of vibrational energy. This may be relevant to the new interaction among individual molecules, for instance the hydrogen bond here. When pressure increases, the interaction energy grows with the compression of distance between molecules. The Gibbs free energy increases rapidly. When it reaches a critical point, the original hydrogen-bond networks cannot be maintained. Then the reconstitution of hydrogen bond occurs in the purpose of reducing the Gibbs free energy.[9,36] The red shifts after frequency drops indicate the bonds soften and the vibrational energy reduces above 8.5 GPa, which are induced by the attractive interaction of new hydrogen bonds.[9,36] In the similar system of tetrazole, Cui's work reported the formation of hydrogen bonds between layers which is accompanied by the distortion of heterocycle, and Raman spectra show similar transformation to red shift with frequency drop through the transition.[9] Similarly, the reported phase transition at 9–15 GPa of urea nitrate in ref. 36 was also influenced by the reconstruction of hydrogen bonds, resulting in a collapse of the initial 2D supramolecular structure to 3D hydrogen-bonded networks. This process also shows transformations from blue shift to red shift in Raman modes. Therefore, we propose that the structural transition at ∼8.5 GPa may relate to the formation of new hydrogen bonds. It can be the source of the NH$_2$ rotation and distortion of the heterocycle in the second phase transition.

In the first and the third transition, although some new peaks show red shifts, including the new peak emerging at 1556 cm^{-1} around 6.6 GPa and the new mode observed at 3166 cm^{-1} near 19.1 GPa. However, there are no obvious drops of frequency near the transition pressure point. It indicates no vibrational energy releases in both phase transitions. We propose that no new hydrogen bonds are formed in the

transitions at 2.3–6.6 GPa and ∼17.7 GPa, and the new peaks with red shifts may be influenced by the original hydrogen bonds.

Conclusions

In conclusion, DAT has phase transitions at the pressure of 2.3–6.6 GPa, ∼8.5 GPa and ∼17.7 GPa. From the results of vibrational spectra and XRD experiment under high pressure, it is indicated that the first phase transition at 2.3–6.6 GPa is relevant to the rotation of NH$_2$; the second phase transition at ∼8.5 GPa and the last phase transition at ∼17.7 GPa are related to both distortion of heterocycle and rotation of NH$_2$. Significantly, the anomalies in the second phase transition may be induced by the reconstitution of hydrogen bonds. Besides, no obvious evidence of the molecular transformation between the two molecular structures is found in the vibration spectroscopy and XRD pattern.

Conflicts of interest

There are no conflicts to declare.

Acknowledgements

Notes and references

1 F. P. A. Fabbiani and C. R. Pulham, High-pressure studies of pharmaceutical compounds and energetic materials, *Chem. Soc. Rev.*, 2006, **35**, 932–942.

2 D. M. Badgujar, M. B. Talawar, S. N. Asthana and P. P. Mahulikar, Advances in science and technology of modern energetic materials: An overview, *J. Hazard. Mater.*, 2007, **151**, 289–305.

3 G. A. Olah and D. R. Squire, *Chemistry of Energetic Materials*, Academic Press, The United State of America, 1991.

4 L. E. Fried, M. RiadManaa, P. F. Pagoria and R. L. Simpson, Design and synthesis of energetic materials, *Annu. Rev. Mater. Res.*, 2001, **31**, 291–321.

5 M. B. Talawar, R. Sivabalan, T. Mukundan, H. Muthurajan, A. K. Sikder, B. R. Gandhe and A. Subhananda Rao, Environmentally compatible next generation green energetic materials (GEMs), *J. Hazard. Mater.*, 2009, **161**, 589–607.

6 P. F. Pagoria, G. S. Lee, A. R. Mitchell and R. D. Schmidt, A review of energetic materials synthesis, *Thermochim. Acta*, 2002, **384**, 187–204.

7 D. Gao, J. Huang, X. Lin, D. Yang, Y. Wang and H. Zheng, Phase transitions and chemical reactions of octahydro-

1,3,5,7-tetranitro-1,3,5,7-tetrazocine under high pressure and high temperature, *RSC Adv.*, 2019, **9**, 5825–5833.

8 S. J. P. Palmer and J. E. Field, The Deformation and Fracture of β-HMX, *Proc. R. Soc. London, Ser. A*, 1982, **383**, 399–407.

9 W. Li, X. Huang, K. Bao, Z. Zhao, Y. Huang, L. Wang, G. Wu, B. Zhou, D. Duan, F. Li, Q. Zhou, B. Liu and T. Cui, A novel high-density phase and amorphization of nitrogen-rich 1*H*-tetrazole (CH₂N₄) under high pressure, *Sci. Rep.*, 2017, **7**, 39249.

10 H. S. Huang, Z. M. Li, G. T. Zhang, T. L. Zhang and W.-H. Hua, Synthesis, crystal structure and thermal synthesis, crystal structure and thermal complex with tetrazole-1-acetic acid, *Main Group Chem.*, 2014, **13**, 117–127.

11 M. I. Eremets, A. G. Gavriliuk, I. A. Trojan, D. A. Dzivenk and R. Boehler, Single-bonded cubic form of nitrogen, *Nat. Mater.*, 2004, **3**, 558–563.

12 M. I. Eremets, M. Y. Popov, I. A. Trojan, V. N. Denisov, R. Boehler and R. J. Hemlev, Polymerization of nitrogen in sodium azide, *J. Chem. Phys.*, 2004, **120**, 10618.

13 D. Laniel, B. Winkler, T. Fedotenko, A. Pakhomova, S. Chariton, V. Milman, V. Prakapenka, L. Dubrovinsky and N. Dubrovinskaia, High-pressure polymeric nitrogen allotrope with the black phosphorus structure, *Phys. Rev. Lett.*, 2020, **124**, 216001.

14 C. Ji, A. A. Adeleke, L. Yang, B. Wan, H. Gou, Y. Yao, B. Li, Y. Meng, J. S. Smith, V. B. Prakapenka, W. Liu, G. Shen, W. L. Mao and H.-K. Mao, Nitrogen in black phosphorus structure, *Sci. Adv.*, 2020, **6**, eaba9206.

15 O. Bolton and A. J. Matzger, Improved stability and smart-material functionality realized in an energetic co-crystal, *Angew. Chem.*, 2011, **123**, 9122–9125.

16 M. Mellini, The crystal structure of lizardite 1T: hydrogen bonds and polytypism, *Am. Mineral.*, 1982, **67**, 587–598.

17 U. Bemm and H. Ostmark, 1,1-Diamino-2,2-dinitroethylene: a novel energetic material with infinite layers in two dimensions, *Acta Crystallogr., Sect. C: Cryst. Struct. Commun.*, 1998, **54**, 1997–1999.

18 D. E. Chavez, M. A. Hiskey and R. D. Gilardi, 3,3'-Azobis(6-amino-1,2,4,5-tetrazine): A novel high-nitrogen energetic material, *Angew. Chem., Int. Ed.*, 2000, **39**(10), 1791.

19 P. Yin, D. A. Parrish and J. M. Shreeve, Energetic multi-functionalized nitramino-pyrazoles and their ionic derivatives ternary hydrogen-bond induced high energy density materials, *J. Am. Chem. Soc.*, 2015, **137**(14), 4778–4786.

20 J. Zhang, Q. Zhang, T. T. Vo, D. A. Parrish and J. M. Shreeve, Energetic salts with π-stacking and hydrogen-bonding interactions lead the way to future energetic materials, *J. Am. Chem. Soc.*, 2015, **137**, 1697–1704.

21 C. Murli, S. M. Sharma, S. Karmakar and S. K. Sikka, α-Glycine under high pressures: A Raman scattering study, *Phys. B*, 2003, **339**, 23–30.

22 A. K. Mishra, C. Murli, N. Garg, R. Chitra and S. M. Sharma, Pressure-induced structural transformations in bis(glycinium)oxalate, *J. Phys. Chem. B*, 2010, **114**, 17084–17091.

23 K. Aoki, H. Yamawaki, M. Sakashita and H. Fujihisa, Infrared absorption study of the hydrogen-bond symmetrization in ice to 110 GPa, *Phys. Rev. B: Condens. Matter Mater. Phys.*, 1996, **54**, 15673–15677.

24 A. S. Lyakhov, P. N. Gaponik and S. V. Voitekhovich, 1,5-Diamino-1*H*-1,2,3,4-tetrazole, *Acta Crystallogr., Sect. C: Cryst. Struct. Commun.*, 2001, **57**, 185–186.

25 A. I. Lesnikovich, O. A. Ivashkevich, S. V. Levchik, A. I. Balabanovich, P. N. Gaponik and A. A. Kulak, Thermal decomposition of amino-tetrazoles, *Thermochim. Acta*, 2002, **388**, 233–251.

26 S. V. Levchik, A. I. Balabanovich, O. A. Ivashkevich, A. I. Lesnikovich, P. N. Gaponik and L. Costa, The thermal decomposition of aminotetrazoles. Part 2.l-Methyl-5-aminotetrazole and 1,5-diaminotetrazole, *Thermochim. Acta*, 1993, **225**, 53–65.

27 M. V. Shakhova, N. V. Muravyev, N. P. Gritsan and V. G. Kiselev, Thermochemistry, Tautomerism, and Thermal Decomposition of 1,5-Diaminotetrazole: A High-Level *ab Initio* Study, *J. Phys. Chem. A*, 2018, **122**(15), 3939–3949.

28 P. N. Gaponik and V. P. Karavai, Synthesis and properties of 1,5-diaminotetrazole, *Chem. Heterocycl. Compd.*, 1984, **20**(12), 1388–1391.

29 D. S. McClure, Optical spectra of transition metal ions in corundum, *J. Chem. Phys.*, 1962, **36**, 2757.

30 J. Eggert, K. Goettel and I. Silvera, Ruby at high pressure. I. Optical line shifts to 156 GPa, *Phys. Rev. B: Condens. Matter Mater. Phys.*, 1989, **40**, 5724.

31 H. K. Mao, J. Xu and P. M. Bell, Calibration of the ruby pressure gauge to 800 kbar under quasi-hydrostatic conditions, *J. Geophys. Res.: Space Phys.*, 1986, **91**, 4673.

32 H. B. Jonassen, T. Paukert and R. A. Henry, Infrared spectra of some 5-aminotetrazole and their deuterated derivatives, *Appl. Spectrosc.*, 1967, **21**(2), 89–91.

33 D. Lin-Vien, N. B. Coulthup, W. G. Fateley and J. G. Grasselli, *The Handbook of Infrared and Raman Characteristic Frequencies of Organic Molecules*, Academic Press, Boston, 1991.

34 J. C. Gálvez-Ruiz, G. Holl, K. Karaghiosoff, T. M. Klapotke, K. Lohnwitz, P. Mayer, H. Noth, K. Polborn, C. J. Rohbogner, M. Suter and J. J. Weigand, Derivatives of 1,5-diamino-1*H*-tetrazole: a new family of energetic heterocyclic-based salts, *Inorg. Chem.*, 2005, **44**, 4237–4253.

35 G. H. Tao, Y. Guo, D. A. Parrish and J. M. Shreeve, Energetic 1,5-diamino-4*H*-tetrazolium nitro-substituted azolates, *J. Mater. Chem.*, 2010, **20**, 2999–3005.

36 S. Li, Q. Li, K. Wang, M. Zhou, X. Huang, J. Liu, K. Yang, B. Liu, T. Cui, G. Zou and B. Zou, Pressure-induced irreversible phase transition in the energetic material urea nitrate: combined Raman scattering and X-ray diffraction study, *J. Phys. Chem. C*, 2013, **117**, 152–159.

37 S. D. Hamann and M. Linton, The influence of pressure on the infrared spectra of hydrogen-bonded solids. IV* miscellaneous compounds, *Aust. J. Chem.*, 1976, **29**, 1825–1827.